Finding Time Period-Based Most Frequent Path in Big Trajectory Data

Wuman Luo, Haoyu Tan, Lei Chen, Lionel M. Ni
Department of Computer Science and Engineering
Guangzhou HKUST Fok Ying Tung Research Institute
Hong Kong University of Science and Technology, Hong Kong SAR, China
{luowuman, hytan, leichen, ni}@cse.ust.hk

ABSTRACT

The rise of GPS-equipped mobile devices has led to the emergence of big trajectory data. In this paper, we study a new path finding query which finds the *most frequent path* (MFP) during user-specified time periods in large-scale historical trajectory data. We refer to this query as *time period-based MFP* (TPMFP). Specifically, given a time period T, a source v_s and a destination v_d, TPMFP searches the MFP from v_s to v_d during T. Though there exist several proposals on defining MFP, they only consider a fixed time period. Most importantly, we find that none of them can well reflect people's common sense notion which can be described by three key properties, namely *suffix-optimal* (i.e., any suffix of an MFP is also an MFP), length-insensitive (i.e., MFP should not favor shorter or longer paths), and bottleneck-free (i.e., MFP should not contain infrequent edges). The TPMFP with the above properties will reveal not only common routing preferences of the past travelers, but also take the time effectiveness into consideration. Therefore, our first task is to give a TPMFP definition that satisfies the above three properties. Then, given the comprehensive TPMFP definition, our next task is to find TPMFP over huge amount of trajectory data efficiently. Particularly, we propose efficient search algorithms together with novel indexes to speed up the processing of TPMFP. To demonstrate both the effectiveness and the efficiency of our approach, we conduct extensive experiments using a real dataset containing over 11 million trajectories.

Categories and Subject Descriptors

H.2.8 [**Database Applications**]: Spatial databases and GIS

Keywords

path finding, big trajectory data

1. INTRODUCTION

In recent years, due to the continuing improvements in location-acquisition technology (e.g., GPS), large amounts of historical trajectory data have become available for emerging applications including urban planning [32], spatio-temporal data mining [17], and various location-based services [29, 31]. Path finding, also known as finding the most desirable path, plays a crucial role in these applications. Traditionally, the *desirability* of a path is usually measured by travel distance or time. In this paper, we study time period-based most frequent path (TPMFP), a new path finding query which aims at **finding the most frequent path of a certain time period**.

The objective of TPMFP is to reflect the common routing preference of the past travelers, which is very useful in many real-world applications. In map services and vehicle navigation systems, TPMFP provides users with extra routing options other than the shortest/fastest path. For example, when traveling in an unfamiliar city, people tend to follow the most common path for several considerations such as making sure that the path is not blocked by a recent road work, reducing the risks of getting lost, and avoiding unpaved roads and dangerous shortcuts. In these situations, a TPMFP such as 'the MFP from my hotel to the airport during the last week' is a better recommendation than the shortest/fastest path. Another application is trajectory data mining where the TPMFP query can be used as a critical subroutine for high-level data analysis. For example, we can find out 'whether people's travel habits during weekends and workdays in the last year are different' by issuing two TPMFP queries (with segmented time periods). It is also possible to detect important events by mining the changes of MFP during different time periods (see Section 6).

Despite that the meaning of MFP is easy to understand, it is non-trivial to give a satisfactory definition to well reflect people's common sense notion. We will illustrate this by a concrete example. Figure 1 shows a road network along with 44 trajectories. The road network is represented by a graph with each vertex being a road intersection and each edge being a road segment. The trajectories are divided into groups according to whether they traverse the same path. As depicted by dashed curves, there are 6 trajectory groups (G_1 through G_6), containing 8, 6, 4, 5, 1, 20 trajectories, respectively. For the ease of presentation, we use v_i–v_j *path/MFP* to denote a path/MFP from v_i to v_j. In this example, we want to find the v_1–v_{12} MFP, assuming that all the trajectories are within the given time period.

A straightforward definition of MFP is to count the number of the trajectories going through each v_1–v_{12} path and select the one with the highest support. In this case, there are four v_1–v_{12} paths with non-zero supports, i.e., the paths traversed by G_1, G_2, G_4, G_5 whose supports are 8, 6, 5, 1, respectively. Hence, the v_1–v_{12} MFP under this definition is $v_1 \rightarrow v_2 \rightarrow v_{12}$. Given the v_1–v_{12} MFP, it is natural to infer that the v_2–v_{12} MFP should be $v_2 \rightarrow v_{12}$, i.e., the suffix of the v_1–v_{12} MFP starting from v_2. However, since the support of path $v_2 \rightarrow v_{12}$ is 8 and the support of path $v_2 \rightarrow v_3 \rightarrow v_{12}$ is $6+4 = 10$, the resulting v_2–v_{12} MFP is the

SIGMOD'13, June 22–27, 2013, New York, New York, USA.

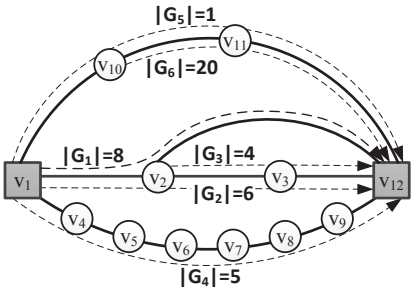

Figure 1: An illustrative example

latter. This result demonstrates that if we use the simple-counting rule to define MFP, then the MFP from an intermediate vertex to the destination is not necessarily a suffix-path of the original MFP. As a consequence, users have to continuously issue queries to a vehicle navigation system to get the MFP starting from the current location, which implies that such a MFP definition is undesirable for practical applications.

Another approach to define MFP is to adopt a scalar-valued score function to calculate path frequency. Initially, each graph edge (or vertex) is associated with a weight or multiple weights calculated from the involved trajectories. Next, an aggregate function is used to calculate a scalar-valued score for each path, taking all the edge (or vertex) weights of a path as input parameters. Then the path with the highest score is considered as the MFP. A possible MFP score function is the sum of all the weights of the edges along the path where the edge weight describes *edge frequency* which is defined as the total number of trajectories passing through the edge. In fact, most existing works related to MFP adopt similar forms of definitions. They only differ in the definition of edge (or vertex) weight (e.g., transfer probability [3]) or the aggregate function for path score calculation (e.g., product [3]).

However, this scalar-valued scoring approach for MFP definition suffers from two major drawbacks. The first drawback is that the number of path edges (path length) can significantly affect the overall path score. For example, it is intuitive that path $v_1 \rightarrow v_2 \rightarrow v_3 \rightarrow v_{12}$ is more frequent than path $v_1 \rightarrow v_4 \rightarrow \cdots \rightarrow v_9 \rightarrow v_{12}$. However, if we adopt the above sum-of-edge-frequency definition, the score of the former $(14 + 10 + 10 = 34)$ is lower than that of the latter $(5 \times 7 = 35)$, which contradicts the intuition. As another example, the definition of *most popular route* (MPR) proposed in [3] tends to favor paths with fewer vertices, which is also undesirable. The reason is that vertex weights are probability values (i.e., $\in [0, 1]$) and the path score is the product of vertex weights. The second drawback is that the resulting MFP may contain very infrequent edges because the weights of infrequent edges can be easily offset by the weights of frequent ones. For example, the score of path $v_1 \rightarrow v_{10} \rightarrow v_{11} \rightarrow v_{12}$ is $1 + 21 + 21 = 43$, which is the highest among all v_1–v_{12} paths. However, we should not consider it as the MFP because there is only 1 trajectory traversing the sub-path from v_1 to v_{10}. This bottleneck suggests that most people have tried to avoid taking it in the past. The possible reasons may be that it is blocked by road work or too dangerous to drive on. Thus, it is undesirable to be included in the MFP.

Aside from the difficulties of proposing a reasonable definition, it is also challenging to process the TPMFP query efficiently in big trajectory data. To the best of our knowledge, we are the first to study the MFP problem with user-specified time periods. In the absence of time periods, most computations (e.g., building the weighted graph) can be performed in an offline manner. In our case, however, massive online computations are inevitable as it is infeasible to compute and store the TPMFP results for all possible time periods. Besides, as the size of a historical trajectory dataset is usually quite large, we do not assume that all data can be loaded into memory. To enable efficient processing of the TPMFP query, it is necessary to devise special index structures to reduce the number of trajectories need to be fetched from disk.

In this paper, we study the problem of TPMFP in big trajectory data. We assume that each trajectory in the dataset has been aligned to the corresponding road network and represents a meaningful trip in the past. To overcome the shortcomings of previous definitions, we use a sequence instead of a single scalar to describe the frequency of a path. We then define a total-order relation to compare path frequencies. To answer TPMFP in a very large dataset efficiently, we design efficient algorithms as well as special index structures. The main contributions of this paper are as follows:

- We propose a time period-based definition of MFP and demonstrate that it is suffix-optimal, length-insensitive, and bottleneck-free (Section 2).
- We propose a two-step framework to solve the TPMFP problem in the context of very large trajectory datasets (Section 3).
- We propose efficient footmark graph construction algorithms along with two novel indexes to significantly reduce the number of disk I/O operations (Section 4).
- We propose efficient algorithms for searching TPMFP on a footmark graph based on the more-frequent-than relation (Section 5).
- We conduct extensive experiments using a real dataset containing over 11 million trajectories to evaluate the performance of our algorithms and indexes. The results show that our approaches are both effective and efficient (Section 6).

We present the related works in Section 7 and conclude the paper in Section 8.

2. THE TPMFP PROBLEM

The problems of the existing definitions and the necessity of allowing user-specified time periods motivate us to seek a novel way to define TPMFP. In particular, we require the definition to satisfy the following three key properties to avoid the aforementioned drawbacks.

PROPERTY 1 (SUFFIX-OPTIMAL). *Let P^* denote the v_s–v_d MFP. For any vertex $u \in P^*$, the sub-path (suffix) of P^* from u to v_d should be the u–v_d MFP.*

PROPERTY 2 (LENGTH-INSENSITIVE). *The length of any path should not be a deciding factor of whether it is the v_s–v_d MFP.*

PROPERTY 3 (BOTTLENECK-FREE). *The MFP P^* should not contain infrequent edges (i.e., bottlenecks).*

In the rest of this section, we present formal definitions for the TPMFP problem and explain why our TPMFP definition satisfies the above properties.

2.1 Sketch of the Problem Definition

Our basic idea is to use a sequence instead of a scalar to describe *path frequency*. We first construct a weighted sub-graph of the road network called *footmark graph* for a given destination v_d and a given time period T. In a footmark graph, the weight of an edge (u, v) is defined as the number of trajectories going through (u, v)

Table 1: Summary of Notations

Notation	Description
G, P, Y	road network, path, trajectory
$V(*)/E(*)$	vertex/edge set of $*$
X	path or trajectory
$X.s/X.d$	starting/ending vertex of X
X_{u-v}	sub-path/sub-trajectory of X from u to v
X_{*-v}	sub-path/sub-trajectory of X from $X.s$ to v
X_{u-*}	sub-path/sub-trajectory of X from u to $X.d$
$X[i]$	the ith element of X
$Y.P$	the corresponding path traversed by Y
$Y.t_s/Y.t_e$	the starting/ending time of Y
Υ	trajectory set
v_s/v_d	source/destination vertex
T	time period
Ω	the input of TPMFP
$\widetilde{Y}_{(v_d,T)}$	the footmark of Y w.r.t. v_d and T
G_f	footmark graph
$\widetilde{\Upsilon}_{(v_d,T)}$	footmark set of Υ w.r.t. v_d and T
$F(u,v)$	frequency of edge (u,v)
$F(P)$	frequency of path P
w_{uv}	weight of edge (u,v)
$\Upsilon_{(v_d,T)}$	trajectories in Υ arriving at v_d within T

and reaching v_d during T, i.e., edge frequency w.r.t. v_d and T. We then define path frequency based on the footmark graph. It is worth emphasizing that since footmark graph is specific to v_d and T, path frequency is also specific to v_d and T. Given a footmark graph G_f and a path $P \subseteq G_f$ (whose ending vertex is v_d), path frequency $F(P) = (f_1, \ldots, f_k)$ is a sequence obtained by sorting all the edge weights of P in non-decreasing order. In other words, f_i is the edge frequency of the ith least frequent edge in P. Consider the example shown in Figure 1. The path frequencies of paths $v_1 \to v_2 \to v_{12}$, $v_1 \to v_2 \to v_3 \to v_{12}$, and $v_1 \to v_{10} \to v_{11} \to v_{12}$ are $(8, 14)$, $(10, 10, 14)$, and $(1, 21, 21)$, respectively. The final step is to define the MFP based on sequence-valued path frequencies. To this end, we define a '*more-frequent-than*' relation ($\succeq$) to compare path frequencies. Given two path frequencies $F = (f_1, \ldots, f_m)$ and $F' = (f'_1, \ldots, f'_n)$, $F \succeq F'$ if F is a prefix of F' or the first f_j, which is different from f'_j, is greater than f'_j. According to this relation, we have $(10, 10, 14) \succeq (8, 14)$ and $(8, 14) \succeq (1, 21, 21)$. Consequently, path $v_1 \to v_2 \to v_3 \to v_{12}$ is considered as the MFP according to our definitions. Note that the non-decreasing ordering of components in path frequency ensures that relation $\succeq$ is a total order, which guarantees the existence of *the highest ranked* path frequency. It is also the key to making the TPMFP definition satisfy the bottleneck-free property. This is because less frequent edges have higher priorities in the comparison of path frequencies.

2.2 Formal Definition

Below we give the formal definitions related to TPMFP. For clarity, the main notations used in the rest of this paper are summerized in Table 1.

DEFINITION 1 (ROAD NETWORK). *A road network is a directed graph $G = (V, E)$ where V is a set of vertices representing road intersections and E is a set of edges representing road segments.*

DEFINITION 2 (PATH). *Given G, an x_1–x_k path is a non-empty graph $P = (V_p, E_p)$ of the form $V_p = \{x_1, x_2, \ldots, x_k\}$ and $E_p = \{(x_1, x_2), \ldots, (x_{k-1}, x_k)\}$ such that P is a sub-graph of G and the x_i are all distinct.*

We use $P.s$, $P.d$, and $P[i]$ to denote the source vertex x_1, the ending vertex x_k, and the ith vertex x_i, respectively. In addition, P is often represented in the form of $x_1 \to x_2, \ldots, \to x_k$.

DEFINITION 3 (TRAJECTORY). *Given G, a trajectory Y is a sequence $((x_1, t_1), (x_2, t_2), \ldots, (x_k, t_k))$ such that there exists a path $x_1 \to x_2, \to, \ldots, \to x_k$ on G and t_i is a timestamp indicating the time when Y passes x_i.*

Similar to path, we use $Y.s$, $Y.d$, $Y[i].v$ and $Y[i].t$ to denote the starting vertex x_1, the ending vertex x_k, the ith vertex x_i and the ith timestamp t_i, respectively. Besides, we use $Y.t_s$, $Y.t_e$, $Y.P$ to denote the starting time t_1, the ending time t_k, and the corresponding path, respectively.

Let $\Omega = (G, \Upsilon, v_s, v_d, T)$ denote the input for the TPMFP problem, where G is a road network, Υ is a set of historical trajectories, $v_s, v_d \in V(G)$ are two vertices indicating the source and destination, respectively, and T is a time period. Without loss of generality, we assume that T is a continuous time period $[t_s, t_e]$, where t_s is the starting time and t_e is the ending time.

In the presence of v_s, v_d, and T, it is obvious that we should only consider the trajectories that can potentially contribute to calculating TPMFP. In specific, we focus on the trajectories that have gone through v_d during T. Note that we do not factor out the trajectories that have not gone through v_s because they can help calculating the parts of the TPMFP starting from intermediate vertices. For example, the trajectory group G_3 (Figure 1) contributes to the frequency of the sub-path from v_2 to v_{12} in searching the v_1–v_{12} TPMFP. Besides, for any trajectory reaching v_d, the sub-trajectory Y_{v_d-*} can be safely discarded because after that point it does not go towards the destination v_d any more (assuming that each trajectory does not traverse a vertex more than once). We summarize the above discussion by presenting the formal definition of footmark.

DEFINITION 4 (FOOTMARK). *Given $\Omega = (G, \Upsilon, v_s, v_d, T)$ and a trajectory $Y = ((x_1, t_1), \ldots, (x_k, t_k)) \in \Upsilon$, if there exists a non-empty sub-trajectory Y' of Y from $Y[i]$ to $Y[j]$ such that:*

- *$Y'.d = v_d$, i.e., $Y[j].v = v_d$,*
- *$[Y'.t_s, Y'.t_e] \subseteq T$, i.e., $[Y[i].t, Y[j].t] \subseteq T$,*
- *$Y[i-1].t \notin T$, if $i > 1$,*

then path $Y'.P$ is the footmark of Y w.r.t. v_d and T, denoted as $\widetilde{Y}_{(v_d,T)}$.

In the following, we abbreviate $\widetilde{Y}_{(v_d,T)}$ as $\widetilde{Y}$ if it is clear from the context. Note that $\widetilde{Y}$ does not exist if Y has not gone through v_d during T. To better understand the definition, a concrete example is given in Figure 2. The input is $\Omega = (G, \Upsilon, v_1, v_8, [t_s, t_e])$, where G is shown in Figure 2(a) and Υ contains 6 trajectories. Figure 2(b) illustrates how to derive the footmarks from the trajectories in Υ. In general, when $\widetilde{Y}$ exists, it is obtained by removing from Y all the prefix elements whose timestamps are not within T and all the suffix elements after v_d. Here, the resulting footmarks are:

- $\widetilde{Y}_1$: $v_2 \to v_7 \to v_8$,
- $\widetilde{Y}_2$: $v_1 \to v_2 \to v_7 \to v_8$,
- $\widetilde{Y}_3$: $v_1 \to v_2 \to v_6 \to v_8$,
- $\widetilde{Y}_4 = \widetilde{Y}_5$: $v_2 \to v_6 \to v_8$.

Note that $\widetilde{Y}_6$ does not exist since it does not traverse v_8. In the following, we use $\widetilde{\Upsilon}_{(v_d,T)}$ (or $\widetilde{\Upsilon}$ for short) to denote a footmark set of Υ.

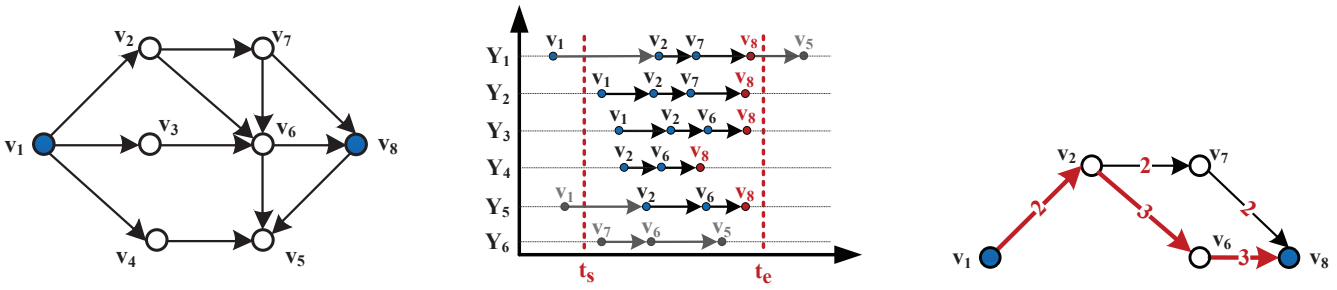

(a) Road network G (b) Footmarks in $\widetilde{\Upsilon}$ (c) Footmark graph G_f

Figure 2: An example of footmark graph for input $\Omega = (G, \Upsilon, v_s, v_d, T)$, where $\Upsilon = \{Y_1, \ldots, Y_6\}$, $v_s = v_1$, $v_d = v_8$, and $T = [t_s, t_e]$

DEFINITION 5 (EDGE FREQUENCY). *Given G, $\widetilde{\Upsilon}_{(v_d,T)}$, and an edge $(u, v) \in G$, the edge frequency $F(u, v)$ is the number of the footmarks in $\widetilde{\Upsilon}_{(v_d,T)}$ containing (u, v).*

In Figure 2(a), for example, $F(v_1, v_2) = 2$ because it is contained by two footmarks, i.e., $\widetilde{Y}_2$ and $\widetilde{Y}_3$.

DEFINITION 6 (FOOTMARK GRAPH). *Given G and $\widetilde{\Upsilon}_{(v_d,T)}$, a footmark graph G_f is a weighted sub-graph of G such that:*

- *for any edge $(u, v) \in G$, $w_{uv} = F(u, v)$;*
- *edge $(u, v) \in G_f$, if and only if $(u, v) \in G$ and $w_{uv} > 0$.*

Figure 2(c) shows the footmark graph for the previous example. Figure 3 illustrates a footmark graph derived from the real dataset used in our experiments. The destination is located at the center of the plot region and the edge frequency is described by the line width where $\mathrm{LineWidth(u, v)} \sim \mathrm{O(log\, F(u, v))}$.

(a) Distant view (b) Close view

Figure 3: A footmark graph derived from a real dataset

Now we define path frequency in terms of edge frequency. The traditional approach is to use an aggregate function such as sum and product to compute a scalar-valued score for each path from the weights of the related edges. The problem is that these functions are not robust such that the resulting MFP tends to be length-sensitive and may contain infrequent edges. To address this issue, we propose a new approach to define path frequency.

DEFINITION 7 (PATH FREQUENCY). *Given G_f, the frequency of path P (to v_d) is a sequence $F(P) = (f_1, \ldots, f_k)$ where:*

- $\{f_i | i \in \{1, \ldots, k\}\} = \{w_{uv} | (u, v) \in E(P)\}$,
- $f_1 \leq f_2 \leq \cdots \leq f_k$.

In other words, $F(P)$ is a non-decreasing sequence of the weights of all the edges in P. For example, the frequency of path $v_1 \rightarrow v_2 \rightarrow v_6 \rightarrow v_8$ in Figure 2(c) is $(2, 3, 3)$ and the frequency of the other v_1–v_8 path is $(2, 2, 2)$.

To define MFP, we further establish a ranking system for sequence-valued path frequencies by defining the more-frequent-than relation.

DEFINITION 8 (MORE-FREQUENT-THAN RELATION). *Given two path frequencies $F(P) = (f_1, \ldots, f_m)$ and $F(P') = (f'_1, \ldots, f'_n)$ w.r.t. the same G_f, $F(P)$ is more-frequent-than $F(P')$, denoted as $F(P) \succeq F(P')$, if one of the following statements holds:*

- *$F(P)$ is a prefix of $F(P')$;*
- *there exists a $q \in \{1, \ldots, \min(m, n)\}$ such that 1) $f_i = f'_i$ for all $i \in \{1, \ldots, q-1\}$, if $q > 1$, and 2) $f_q > f'_q$.*

Particularly, $F(P)$ is strictly-more-frequent-than $F(P')$, denoted as $F(P) \succ F(P')$, if $F(P) \succeq F(P')$ and $F(P) \neq F(P')$.

According to the definition, we have $(10, 10, 10) \succeq (1, 100)$, $(1, 2) \succeq (1, 2, 3)$, and $(5, 6, 9) \succeq (5, 6, 7, 12)$, to name a few instances. Essentially, the more-frequent-than relation is a special form of the lexicographic order, which directly leads to the following theorem.

THEOREM 1. *The more-frequent-than relation is a total order.*

The above theorem implies that we can safely define the MFP as the path with the highest ranked frequency.

DEFINITION 9 (MFP). *Given G_f and a v_s–v_d path $P^* \subseteq G_f$, if $F(P^*) \succeq F(P)$ holds for every v_s–v_d path $P \subseteq G_f$, then P^* is the v_s–v_d MFP w.r.t. G_f.*

Finally, we can define the TPMFP problem based on the above definitions.

Problem Statement: Given $\Omega = (G, \Upsilon, v_s, v_d, T)$ where Υ is a very large set of historical trajectories, we need to find the TPMFP which is the MFP w.r.t. G_f. Note that G_f is the footmark graph derived from Ω.

2.3 Properties

Now we explain why the TPMFP definition satisfies the three key properties. We begin with a theorem which demonstrates its suffix-optimal property (due to the page limitation, we omit the lengthy proof).

Algorithm 1: Two major steps for the TPMFP query

Input: $\Omega = (G, \Upsilon, v_s, v_d, T)$
Output: the TPMFP w.r.t. Ω
begin
1 step 1: build the footmark graph G_f w.r.t. Ω ;
2 step 2: find the MFP P^* from v_s to v_d on G_f ;
3 return P^* ;

THEOREM 2. *Given $\Omega = (G, \Upsilon, v_s, v_d, T)$, let P^* be the v_s–v_d TPMFP w.r.t. Ω. Then, for every vertex $u \in V(P)$, the sub-path of P^* from u to v_d is the u–v_d TPMFP.*

The implications of the above theorem are two-fold. First, it ensures the stability of the TPMFP in the sense that the query result from any intermediate location to the destination will not deviate from the initial route, which is desirable for practical applications. Second, it guarantees the existence of efficient (polynomial-time) algorithms to compute the exact result of TPMFP, which is important for time-critical services.

In addition, the TPMFP is length-insensitive and bottleneck-free as well. This is a direct result of the definition of path frequency and the comparison rule. Specifically, given two paths P and P', P is more frequent than P' as long as $F(P)$ wins $F(P')$ in the comparison between their first different components. In other words, the path length is not a deciding factor in such comparisons, which is in line with the common sense that the road segments in a frequent path can be either few or many. For the bottleneck-free property, it is straightforward to prove that if P is the TPMFP, then for any edge $(u, v) \in P$, there does not exist any other path P' such that all edge frequencies of P' are greater than the frequency of (u, v). It implies that the TPMFP does not contain any (infrequent) edge that can be avoided by introducing more frequent ones only.

3. SOLUTION OVERVIEW

Given input $\Omega = (G, \Upsilon, v_s, v_d, T)$, we perform the TPMFP query in two major steps, as illustrated in Algorithm 1.

For the first step, since the edge weights on a footmark graph depend on the input time period T, we cannot calculate them in an offline manner. This fact poses great challenges on building the footmark graph, especially in the presence of huge amounts of trajectories. Assume that the data are stored in a disk-based key-value storage system and a trajectory can be fetched based on its id. A straightforward approach to build a footmark graph is to scan all the trajectories in Υ and update the footmark graph G_f during the process. Initially, G_f is an empty graph. For each trajectory Y being scanned, we first check whether it generates a footmark $\widetilde{Y}$. If so, we update the footmark graph by incrementing the weight of each edge in $E(\widetilde{Y})$ by 1 (if the edge does not exist in G_f, we simply add it to G_f and set its weight to 1). The construction of G_f is completed once all trajectories are processed. However, this approach is inefficient from the perspectives of both I/O and computation: the number of trajectories need to be fetched is $|\Upsilon|$ and the computation complexity for edge weight update is $O(|\widetilde{\Upsilon}| \times l)$, where l is the average length of footmarks. To speed up I/O, we propose *Footmark Index* (FMI) to effectively filter out the trajectories having no footmarks. We further devise *Containment-Based Footmark Index* (CFMI), an improved version of FMI, to further reduce the random page accesses by only fetching the 'dominant' trajectories. To speed up computation, we develop efficient algorithms based on the proposed indexes which dramatically reduces the cost of updating G_f. We will discuss the footmark graph construction in detail in Section 4.

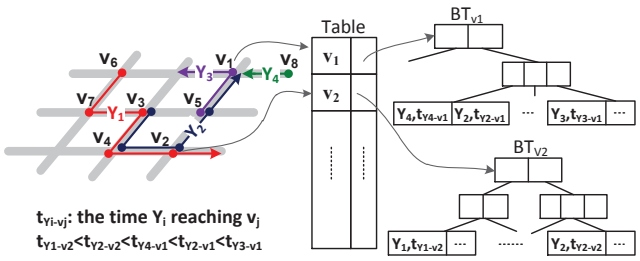

Figure 4: An example of FMI

The second step is described in Section 5. We first prove that searching MFP on a given footmark graph can be solved by the dynamic programming approach. Then we propose a new variant of the classic Bellman–Ford algorithm to deal with the sequence-valued path frequencies. We also demonstrate the correctness of the algorithm and analyze its time and space complexities.

4. FOOTMARK GRAPH CONSTRUCTION

The main task of footmark graph construction is to calculate the footmark set $\widetilde{\Upsilon}$ w.r.t. G, Υ, v_d, and T. As mentioned before, it is inefficient to examine all the trajectories because only a small portion of them have footmarks for the specific v_d and T. In addition, the large number of weight updating operations can lead to high computation cost. As such, we propose two special indexes to reduce disk reads together with efficient algorithms to construct G_f. Note that we assume that all the trajectories are stored on disk and each trajectory can be fetched using one random page read.

4.1 Footmark Index

To calculate $\widetilde{\Upsilon}$, we need to find the trajectories in Υ that have footmarks for the given v_d and T in the first place. To filter trajectories by v_d and T, we design an index called Footmark Index (FMI).

In FMI, we build a B$^+$-tree BT_{v_i} for each vertex $v_i \in V(G)$. BT_{v_i} indexes the time of the trajectories reaching v_i and stores the corresponding trajectory id's. Each leaf entry of BT_{v_i} is of the form $\langle tid, t_a \rangle$, where tid is the unique id of a trajectory, and t_a is the time trajectory tid reaching v_i. Besides, we keep a table in FMI to map each vertex to its corresponding B$^+$-tree. Figure 4 illustrates an example of FMI. Since Y_2 traversed both v_1 and v_2, $\langle Y_2, t_{Y_2\text{-}v_1} \rangle$ and $\langle Y_2, t_{Y_2\text{-}v_2} \rangle$ are the leaf entries in BT_{v_1} and BT_{v_2}, respectively.

Let $|\Upsilon|$ and $|Y|_{max}$ denote the number and the maximum length of the trajectories in Υ, respectively. We can easily derive that the storage space consumed by FMI is $O(|\Upsilon| \times |Y|_{max})$.

Algorithm 2 illustrates the process of footmark graph construction using FMI. FMI-Search(v_d, T) (line 2) is the searching process in FMI. Let $\Upsilon_{(v_d,T)}$ denote the set of all the trajectories arriving at v_d during T. Given v_d and T, FMI-Search(v_d, T) returns the id's of all the trajectories in $\Upsilon_{(v_d,T)}$ via searching BT_{v_d}. To calculate the footmarks, we further examine the elements of each $Y \in \Upsilon_{(v_d,T)}$ (line 3–11). Besides, we build a $|V(G)| \times |V(G)|$ matrix FG whose entries are initialized to zeros. For each newly acquired edge $(vid, vid') \in \widetilde{Y}$, the corresponding entry $FG[vid][vid']$ is incremented by 1 (line 10). In this way, we calculate and record the edge weights of the target footmark graph in FG which is finally returned as the output.

Algorithm 2: FMI-FG(v_d, T)

```
   begin
1      FG ← |V(G)| × |V(G)| matrix with all entries zeros ;
2      TRID ← FMI-Search(v_d, T) ;
3      for each tid ∈ TRID do
4          Y ← GetTraj(tid) ;
5          (vid, t) ← the first element of Y ;
6          while t ∉ T do
7              (vid, t) ← the next element of Y ;
8          while vid ≠ v_d do
9              (vid', t') ← the next element of Y ;
10             FG[vid][vid'] ← FG[vid][vid'] + 1 ;
11             (vid, t) ← (vid', t') ;
12     return FG ;
```

Let Υ_{v_d} denote the set of all the trajectories traversing v_d. Then the cost of FMI-Search(v_d, T) is $O(log(|\Upsilon_{v_d}|) + |\Upsilon_{(v_d,T)}|)$. After fetching the trajectories from disk, the algorithm calculates the footmark graph in $O(|\Upsilon_{(v_d,T)}| \times |Y|_{max})$ time. Note that the performance bottleneck of Algorithm 2 is the I/O cost caused by trajectory fetching in GetTraj(tid) (line 4). Specifically, for each returned tid, the corresponding trajectory needs to be transferred from the disk, incurring $|\Upsilon_{(v_d,T)}|$ random page reads in total.

4.2 Containment-Based Footmark Index

Although FMI can prune all the trajectories not in $\Upsilon_{(v_d,T)}$, it incurs $|\Upsilon_{(v_d,T)}|$ page accesses. To further reduce the number of random reads, we improve FMI by organizing the involved trajectories into different groups. In each group, the front part of each trajectory Y before reaching v_d (including v_d), denoted as Y_{*-v_d}, is 'contained' by a unique 'dominant' trajectory. As a result, we only need to fetch the 'dominant' trajectory and calculate the footmarks of the contained ones by simply recording their starting locations w.r.t. the 'dominant' trajectory. We refer to this new index as Containment-Based Footmark Index (CFMI).

DEFINITION 10 (v_d-CONTAINMENT). *For two trajectories Y and Y' in Υ_{v_d}, if $Y_{*-v_d}.P$ is a sub-path of $Y'_{*-v_d}.P$, then Y is v_d-contained by Y'. In particular, if $Y_{*-v_d}.P \neq Y'_{*-v_d}.P$, then Y is strictly v_d-contained by Y'.*

DEFINITION 11 (v_d-DOMINANT). *A trajectory $Y \in \Upsilon_{v_d}$ is v_d-dominant if there exists no $Y' \in \Upsilon_{v_d}$ such that Y is strictly v_d-contained by Y'.*

If there are multiple v_d-dominant trajectories in Υ which are v_d-contained by each other, we pick one of them as v_d-dominant and treat the rest as normal trajectories. As such, each $Y \in \Upsilon_d$ is v_d-contained by exactly one v_d-dominant trajectory. Consider the example in Figure 4. We have $\Upsilon_{v_2} = \{Y_1, Y_2\}$, $Y_{1\,*-v_2}.P = v_6 \rightarrow v_7 \rightarrow v_3 \rightarrow v_4 \rightarrow v_2$, and $Y_{2\,*-v_2}.P = v_3 \rightarrow v_4 \rightarrow v_2$. Obviously, Y_2 is v_2-contained by Y_1 and Y_1 is v_2-dominant in Υ_{v_2}. This means that Y_2 follows the sub-path of Y_1 when traveling to v_2. Hence, we only need to fetch Y_1 to calculate both $\widetilde{Y}_1$ and $\widetilde{Y}_2$ by simply recording the starting location of Y_2 in Y_1. Similarly, Y_2 and Y_4 are both v_1-dominant in Υ_{v_1}.

The basic idea of CFMI is to try to adopt the v_d-dominant trajectories to calculate $\widetilde{\Upsilon}$. This is motivated by the following two observations. First, the number of the v_d-dominant trajectories in Υ_{v_d} tends to be much smaller than $|\Upsilon_{v_d}|$. In other words, the path to v_d taken by a v_d-dominant trajectory is usually (partially) followed by many other trajectories. As we will show in Section 6, this is indeed the case in many real-world scenarios. Second, the range of T is often much larger than the time spans of the trajectories. This means that the starting time of most of the trajectories in $\Upsilon_{(v_d,T)}$ are within T. Thus, we only need to fetch their v_d-dominant trajectories to calculate the corresponding footmarks.

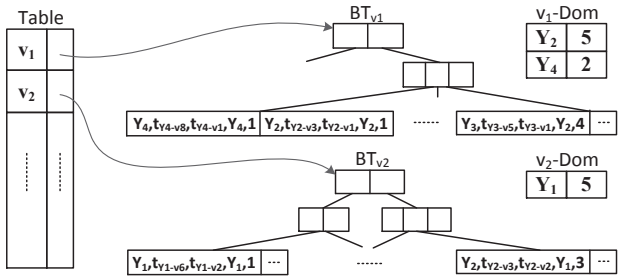

Figure 5: An example of CFMI

CFMI improves the structure of each B$^+$-tree in FMI. Specifically, each leaf entry of BT_{v_i} is in the following new form:

$$\langle tid, t_s, t_a, did, sloc \rangle ,$$

where t_s is the starting time of trajectory tid, did is the id of the v_i-dominant trajectory of trajectory tid, and $sloc$ is the starting location of trajectory tid in trajectory did. Besides, we keep a table v_i-Dom for each BT_{v_i}, in which we record the length of $Y_{*-v_i}.P$ for each v_i-dominant trajectory Y.

Figure 5 illustrates the CFMI for the example in Figure 4. Consider BT_{v_2}. Since Y_1 is the v_2-dominant trajectory, its did equals to its tid. Besides, the $sloc$ of Y_2 is 3 since the starting location of Y_2, i.e., v_3, is the third location traversed by its v_2-dominant trajectory Y_1. In v_2-Dom, the length of $Y_{1\,*-v_2}.P$ is recorded, which equals to the number of the vertices in $Y_{1\,*-v_2}.P$.

Now, we use this example to illustrate the process of the footmark graph construction (Algorithm 3). Suppose the destination is v_1 and only Y_2 and Y_3 arrive at v_1 during T. Then CFMI returns two sets via searching BT_{v_1} and v_1-Dom (line 2): 1) $TRREC = \{(tid, t_s, did, sloc)\}$, which records the information of trajectories in $\Upsilon_{(v_d,T)}$, and 2) $DOM = \{(did, len)\}$, which records the did's appeared in $TRREC$ and their corresponding values in v_1-Dom. In this example, $TRREC$ contains two elements, namely $(Y_2, t_{Y_2\text{-}v_3}, Y_2, 1)$ and $(Y_3, t_{Y_3\text{-}v_5}, Y_2, 4)$. And DOM contains one element, namely $(Y_2, 5)$. Note that Y_4 is not in DOM because it is not returned as a did in any elements of $TRREC$. To calculate the footmarks, we create an array with length len for each entry (did, len) in DOM and organize them in a structure DA (line 3–6). Initially, the elements in each array are set to zeroes. In this example, DA contains only one array $DA.Y_2$ with length 5. Next, for each $(tid, t_s, did, sloc)$ in $TRREC$, we examine whether t_s is in T. Assume that this is true for both Y_2 and Y_3. Then we get $Y_2.did$ and $Y_3.did$, both of which point to Y_2. Further, we find the array $DA.Y_2$ and increment the values of $DA.Y_2[Y_2.sloc]$ and $DA.Y_2[Y_4.sloc]$ by one (line 10), respectively. Note that $DA.Y_2[i] = k$ means that the sub-path of $Y_2.P$ from the ith vertex to v_1 has been traversed by k trajectories during T. In this way, we record the footmarks of the trajectories in the arrays of DA.

Then, we adopt $DA.Y_2 = [1, 0, 0, 1, 0]$ to calculate the footmark graph. Specifically, we fetch Y_2 from disk and do the following calculation (line 11-21). Since $DA.Y_2[1] = 1$, the first edge (v_3, v_4) of $Y_2.P$ has been traversed once. Thus, $FG[v_3][v_4] = 1$. Since

Algorithm 3: CFMI-FG(v_d, T)

```
   begin
1      FG ← |V| × |V| matrix with all entries zeros ;
2      (TRREC, DOM) ← CFMI-Search(v_d, T) ;
3      DA ← ∅ ;
4      for each (did, len) ∈ DOM do
5          create array DA.did[len] with all entries zeros ;
6          DA ← DA ∪ DA.did[len] ;
7      for each (tid, t_s, did, sloc) ∈ TRREC do
8          if t_s ∉ T then
9              Modify-FG(tid) ;
           else
10             DA.did[sloc] ← DA.did[sloc] + 1 ;
11     for each (did, len) ∈ DOM do
12         Y ← GetTraj(did) ;
13         vid ← the first location of Y.P ;
14         k ← 1, w ← 0 ;
15         while vid ≠ v_d do
16             vid' ← the next location of Y.P ;
17             if DA.did[k] ≠ 0 or w ≠ 0 then
18                 w ← w + DA.did[k] ;
19                 FG[vid][vid'] ← FG[vid][vid'] + w ;
20             k ← k + 1 ;
21             vid ← vid' ;
22     return FG ;
```

$DA.Y_2[2] = 0$ and $DA.Y_2[3] = 0$, no more trajectories have traversed the next two edges. We have $FG[v_4][v_2] = FG[v_2][v_5] = 1$. Besides, $DA.Y_2[4] = 1$ means that one more trajectory has traversed the 4th edge. It follows that $FG[v_5][v_1] = 2$. Since v_1 is reached, the calculation is over. Note that there are a small portion of trajectories whose starting time is not in T. To record their footmarks in FG, we read each of them from the disk and follow the lines 4–11 in Algorithm 2 (i.e., Modify-FG(tid) in line 9).

Compared with FMI, CFMI calculates DOM in an extra cost of $O(|\Upsilon_{(v_d,T)}|log|\Upsilon_{(v_d,T)}|)$. However, CFMI is more preferable due to two performance gains. First, instead of fetching each involved trajectories from the disk, CFMI only fetches their dominant ones. Random page reads are therefore largely reduced. Second, instead of checking the elements for each involved trajectory, CFMI records their $sloc$'s in the arrays and examines the dominant ones instead. Thus, the performance of computation is improved.

5. SEARCHING THE TPMFP

So far, we have constructed the footmark graph G_f w.r.t. $\Omega = (G, \Upsilon, v_s, v_d, T)$, where each edge (v_i, v_j) in G_f is associated with a positive weight w_{ij}. The value of w_{ij} stands for the number of the trajectories in Υ that have reached v_d via edge (v_i, v_j) during T. Given G_f, we now proceed to the problem of searching the MFP from v_s to v_d on G_f, namely the TPMFP w.r.t. Ω. In this section, we first prove that the MFP is a simple (acyclic) path on G_f (Lemma 1 and Lemma 2). Base on this result, we then demonstrate that the problem has a recurrence structure that can be solved by dynamic programming (Lemma 3). Finally, we propose an efficient MFP searching algorithm to deal with sequence-valued path frequencies. Note that our algorithm has a similar structure to the Bellman-Ford algorithm.

LEMMA 1. *Let $u \rightsquigarrow v$ denote a path from u to v. Suppose $P^c = v_s \rightsquigarrow v_k \rightsquigarrow v_k \rightsquigarrow v_d$ is a path with cycles on G_f. We have $F(P) \succ F(P^c)$, where P is the resulting path after removing the portion of P^c between consecutive visits to v_k.*

PROOF. Let $P^c_{v_k}$ be the cycle $v_k \rightsquigarrow v_k$ on P^c and w^* the first component of $F(P^c_{v_k})$. Let $F(P) = (w_1, \ldots, w_n)$. Thus, $w_1 \leq \cdots \leq w_n$. Consider the following three cases:

- $w^* < w_1$: in this case, w^* is the first component of $F(P^c)$ as well. Since w_1 is the first component of $F(P)$, we have $F(P) \succ F(P^c)$.
- $w_1 \leq w^* < w_n$: let $w_i \in F(P)$, $1 < i \leq n$, such that $w_{i-1} \leq w^* < w_i$. Thus, the first $i-1$ components of $F(P^c)$ are the same as those of $F(P)$. Note that w^* and w_i are the ith elements of $F(P^c)$ and $F(P)$, respectively. Hence $F(P) \succ F(P^c)$.
- $w_n \leq w^*$: in this case, $F(P)$ is the prefix of $F(P^c)$. Hence $F(P) \succ F(P^c)$.

In summary, we have $F(P) \succ F(P^c)$. □

LEMMA 2. *Given G_f w.r.t. Ω, there exists an MFP from v_s to v_d that is simple, i.e., has at most $|V_f| - 1$ edges.*

PROOF. Since adding a cycle does not make a path more frequent, the v_s–v_d MFP P^* with the fewest number of edges does not repeat any vertex. If P^* did repeat v, we could remove the cycle $v \rightsquigarrow v$, resulting in a more frequent path with less edges. □

Let $F^*(v_s, i)$ be the frequency of the v_s–v_d MFP using at most i edges. By Lemma 2, the frequency of the v_s–v_d MFP is $F^*(v_s, |V_f|-1)$. Let P^* be the v_s-v_d MFP. If P^* uses at most $i-1$ edges, then

$$F^*(v_s, i) = F^*(v_s, i-1) .$$

Besides, by Theorem 2, if P^* uses i edges and the first edge is (v_s, v), we have

$$F^*(v_s, i) = (w_{v_s v}) + F^*(v, i-1) ,$$

where the operator '$+$' is defined as follows:

- If the two inputs are non-decreasing sequences of positive integers, "$+$" merges them into a non-decreasing sequence. For example: $(20) + (5, 20) = (5, 20, 20)$;
- If one input is $\emptyset$, then the other input is returned. If both inputs are $\emptyset$'s, then $\emptyset$ is returned. For example: $\emptyset + (5, 20) = (5, 20)$;
- If one input is $\#$, then $\#$ is returned. For example: $\# + (5, 20) = \#$.

We use $\emptyset$ and $\#$ to represent the frequencies of *empty path* ($v_s = v_d$) and *null path*, respectively. For completeness, we define $\emptyset$ and $\#$ as the highest and the lowest ranked path frequencies, respectively.

Let $Z = (F_1, F_2, \ldots, F_n)$ be an ordered sequence of path frequencies under the $\succeq$ relation, namely $F_1 \succeq F_2 \succeq \cdots \succeq F_n$. Moreover, we define the maximum function over Z as $\max(Z) = F_1$. Thus, we can recursively express $F^*(v_s, |V_f| - 1)$ in smaller sub-problems.

LEMMA 3. *Given $G_f = (V_f, E_f)$, if $i > 0$, then we have*

$$F^*(v_s, i) = max(F^*(v_s, i-1), \max_{(v_s,v) \in E_f}((w_{v_s v}) + F^*(v, i-1))) .$$

Algorithm 4: MFP$(v_s, G_f = (V_f, E_f))$

```
   begin
1      for each u ∈ V_f do
2          if u = v_d then
3              u.ξ ← ∅ ;
4          else
5              u.ξ ← #, u.suc ← null ;
6      P* ← null ;
7      if v_s ∈ V_f then
8          for i ← 1 to |V_f| − 1 do
9              for each edge (u, v) ∈ E_f do
10                 if (w_uv) + v.ξ ≻ u.ξ then
11                     u.ξ ← (w_uv) + v.ξ ;
12                     u.suc ← v ;
13         create P* by following the successors from v_s to v_d ;
14     return P* ;
```

Based on this recursive formula, we design a dynamic programming algorithm to calculate MFP (Algorithm 4). In particular, for each $u \in V_f$, we use $u.\xi$ to record $F^*(u, i)$ found so far. Initially, we set $u.\xi = \#$, if $u \neq v_d$, and $u.\xi = \emptyset$, otherwise (line 1–5). This means that the u–v_d MFP using zero edge does not exist unless $u = v_d$. To help with recovering the MFP, we maintain the next vertex of u in the u–v_d MFP (found in every step) in $u.suc$. At the beginning, we set $u.suc = null$ (line 5). Then, for i iterates from 1 to $|V_f| - 1$ (from line 7), we calculate the u–v_d MFP using the recurrence formula in Lemma 3. The inner for loop (from line 8) is used to calculate the value of $\max_{(v_s,v)\in E_f}((w_{v_s v}) + F^*(v, i-1))$ and update $u.\xi$ as well as $u.suc$ if the u–v_d MFP is changed. Finally, we return the v_s–v_d MFP by sequentially retrieve the vertices along the successor links from v_s to v_d.

The correctness of Algorithm 4 follows directly by induction from the recursive formula in Lemma 4. Assume that the average number of vertices of all the MFP to v_d is α. Then Algorithm 4 calculates the v_s–v_d MFP in time $O(\alpha|V_f||E_f|)$ and requires $O(\alpha|V_f|)$ working memory (note that $\alpha \ll |V_f|$).

In real scenarios, one may start from a position along an edge instead of a vertex, or some vertex via which no trajectories has traversed to the specified destination. One possible solution is to retrieve this position's k-nearest neighbors that are in G_f, calculate the MFP to v_d from these k vertices, and return the most frequent one. Note that k is a user-specified parameter. This augmented algorithm has the same computational complexity as the original one.

6. EVALUATION

We use a real dataset to conduct the experiments. In this section, we first describe the dataset, the experiment environment and some implementation details. Then we analyze the effectiveness of the TPMFP query and the differences between TPMFP and MPR [3] by concrete examples. Finally, we present the evaluation results of the efficiency of our proposed indexes and algorithms.

6.1 Experiment Settings

6.1.1 Dataset

We conduct our experiments on a real dataset containing over 0.5 billion GPS records. These GPS records are collected from around 6,000 taxies in Shanghai in 2007. Along with time and location, each record has an attribute indicating whether the taxi is empty or occupied at that time. We use this attribute to extract meaningful trips of passengers and treat each trip as a single trajectory. This preprocessing technique is also used in [32]. Then we perform a specially tuned map-matching algorithm derived from [18] to align all trajectories to Shanghai's digital map which contains 22,180 vertices and 65,510 edges. After map-matching, each trajectory is represented in the form defined in Section 2.

The preprocessed dataset consists of 11,547,611 trajectories. The total number of vertices is 245,276,717 and the average trajectory length (in terms of the number of vertices) is 21. For each trajectory, the storage size of the trajectory id, the time and the vertex id is 18 bytes, 8 bytes and 4 bytes, respectively. We can see that the dataset is very large and that the all-in-memory techniques are no longer applicable. Since some algorithms may use too much memory or take too long to finish, we also create two subsets of the original data containing the trajectories of a month and a day, respectively. For clarity, we name these datasets as Year Dataset, Month Dataset and Day Dataset. A summary of the datasets is given in Table 2.

Table 2: Summary of Datasets

Dataset Name	No. of Trajectories	Total Length	Size (MB)
Year Dataset	11,547,611	245,276,717	3,335
Month Dataset	1,650,134	35,619,454	484
Day Dataset	54,579	1,217,890	17

6.1.2 Implementation

We implement all our algorithms in Java. The FMI and CFMI indexes are stored as regular files. To handle big datasets, we develop a compact file format optimized for both sequential full scan and single trajectory retrieval.

To compare with MPR, we also implement the related algorithms in [3]. As we have a digital map on hand, we skip the steps of generating a road network from raw trajectories. We believe this change is acceptable as it makes the results more realistic. For our implementation of MPR, most algorithms are written in Java except that matrix operations are written in R. We do so because R is much more efficient than Java in manipulating matrices.

6.1.3 Experiment Environment

We perform all evaluations using a single server. It has a quad-core Intel(R) Xeon(R) E5506 CPU (2.13GHz), 12GB memory and 10,000RPM sever-level hard disks. The operating system is Linux 2.6.32 x86_64 and the Java VM version is 1.7.0_4 64-Bit.

6.2 Effectiveness

To evaluate the effectiveness, we compare the results of four path finding queries, namely TPMFP (or MFP when T is fixed), MPR (Most Popular Route), STP (shortest path) and LRS (path with the least number of road segments). LRS represents the paths with minimum number of hops and it can be easily calculated using any shortest path algorithm by setting all edge weights to 1. Note that the calculations of STP and LRS do not need any trajectories. For TPMFP and MPR, if not otherwise specified, we use Year Dataset and the time period is fixed to the whole year of 2007 (as if T is $[0, +\infty)$).

6.2.1 General Comparison

The very first question we are curious about is whether these queries always find the same paths. To examine this, we fix the des-

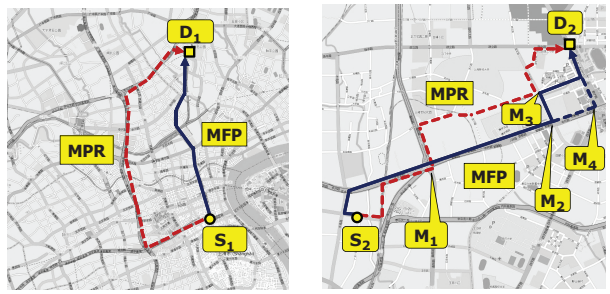

(a) Case 1 (b) Case 2

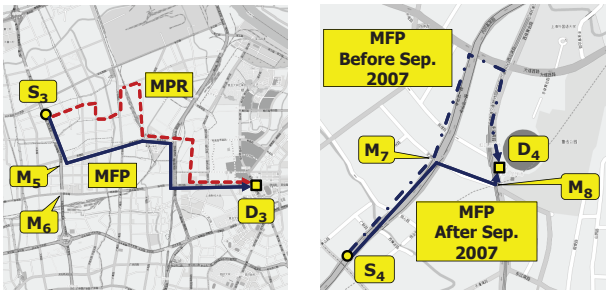

(c) Case 3 (d) Case 4

Figure 6: Examples illustrating the effectiveness of TPMFP

tination and perform the above path finding algorithms over Month Dataset with all possible source vertices. The relations between MFP, MPR and STP are shown in Figure 7(a). We can see that over 80% of the results are pairwise different, which implies that each of them has unique significance and cannot be effectively replaced by others. Another notable fact is that the number of MFPs matching the STP is approximately twice the number of MPRs matching the STP. We do not include LRS in this comparison because LRS always has multiple resulting paths.

As we have mentioned before, the MPR algorithm is prone to select paths with fewer vertices. The reason is that the popularity score of a path is the product of the weights ($\in [0, 1]$) of all vertices along the path. The experiment result also confirms this inference, as is shown in Figure 7(b). There are over 90% of MPRs are also LRSs. In other words, even if a path is taken by most travelers, it has little chance to be chosen by the MPR algorithm if it contains many more vertices than other less frequently used paths. In contrast, there are less than 10% of the MFPs overlapped with LRSs. Therefore, we can safely conclude that *MFP is much more length-insensitive than MPR*.

6.2.2 *Case Study*

Below we conduct several case studies to exhibit the effectiveness of the TPMFP query. One thing worth noting is that there is neither any ground truth of *truly* frequent paths nor any widely-accepted definitions of it, the analysis below might be more or less subjective. Despite that, we believe they do give some strong arguments of why the TPMFP query are useful.

In Figure 6, the first three examples use Month Dataset and the last example uses Year Dataset.

In Figure 6(a), the MPR consists only a few number of road segments, most of which are viaducts or high-speed roads; while the MFP consists of many road segments of regular roads. Though in this case the MPR may be faster than MFP, we notice that the MFP is more direct and its travel distance is much smaller than that of

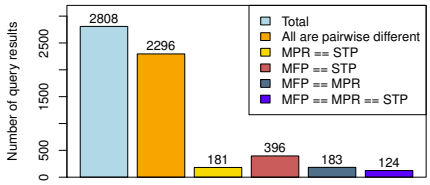

(a) vs. shortest path

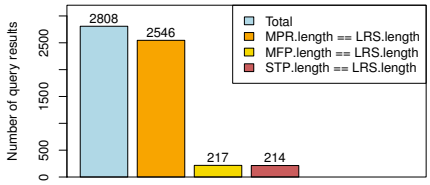

(b) vs. least road segments

Figure 7: Statistics of query results w.r.t a fixed destination

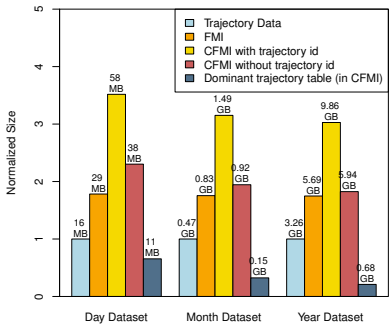

Figure 8: Index size

the MPR. Moreover, we find that there does exist several trajectories traveling along the MFP; whereas there is no trajectory traveling along the MPR in Month Dataset. Based on these observations, we believe most drivers would choose the more direct path as our approach suggests.

In Figure 6(b), the MFP and the MPR have almost the same travel distance. However, the MPR is much more winding than the MFP and it contains many small roads. We cannot find any good reason for a driver to enter the main road, leave at exit M_1 a very short time later, and then spend most of his/her trip on twisted small roads. Indeed, we find that the MPR has one less vertex than the MFP. In fact, this little difference plays a decisive role in the MPR algorithm. If we increase the weight of an arbitrary vertex along the MFP to 1, then the MPR algorithm will result in the same path as the MFP. Another interesting observation is that the MFP is the one through M_3 instead of the one through M_4 (which would be a more direct path). By checking the data, we find out that there is no significant difference between these two paths as the path frequencies are close to each other. To demonstrate this, we perform the TPMFP query with different time periods (e.g., different days or weeks in the same Month Dataset) and find that they have fairly equal chances of being returned as the MFP.

In Figure 6(c), the MPR contains too many twists and turns while the shape of the MFP is much nicer. There is no clear reason making us believe that many past travelers would take the former instead of the latter. The interesting thing here is why the MFP turns

left at M_5 instead of M_6. We discover that the sub-path of the MFP from S_3 to M_5 is a high-speed road and there is no exit at M_6. Therefore, most drivers would exit the high-speed road at M_5 when traveling to D_3.

We perform many TPMFP queries with various time periods and try to discover the changes of the MFP. Figure 6(d) is a representative result, in which the MFP from S_4 to D_4 changes around September 2007. By searching the web we discover that the road between M_7 and M_8 is under construction before then. This example demonstrates that time period-based MFP can be more useful than MFP with a fixed time period.

6.3 Efficiency

In this section, we evaluate the performance of the indexes, the footmark construction algorithms and searching the MFP on a footmark graph.

6.3.1 Index Creation

The creation of FMI and CFMI consists of two steps. First, we create a file for each vertex recording all the trajectories traversing it. This step can be performed efficiently with a single pass of scanning all trajectories. Second, we process each of the resulting files to build FMI or CFMI. For FMI, it is sufficient to sort the records by the arrival time and then pack a B+tree on disk. For CFMI, we use a nested-loop algorithm to calculate the dominant trajectories before building the index. Specifically, we first sort all the trajectories in the same file by length in descending order. Then we iterate over all these trajectories in the sorted order and mark a trajectory as a dominant one if it is not dominated by any of the dominant trajectories found so far. For Year Dataset, the index creation time of FMI and CFMI is 72 minutes and 127 minutes, respectively. Since we only need to create the index once, the speed of the index building algorithms is acceptable.

6.3.2 Index Size

Figure 8 shows the total storage size of different indexes. The size of FMI is slightly smaller than twice of the data size. The size of CFMI is about three times of the data size. Note that we can further improve the space efficiency of CFMI by removing the trajectory id's in the tree structure because they are not used when constructing footmark graphs using CFMI. As a result, the size of CFMI is reduced by 40%. Moreover, we discover that the ratio of the size of the dominant trajectory table in CFMI to the total size of CFMI decreases as the data size grows.

Figure 9 illustrates the decreasing trend of the percentage of dominant trajectories of a representative vertex as more trajectories are added. The result shows that when there are 150,000 trajectories passing through the vertex, we only need to fetch 10% of the trajectories from disk. Figure 10 shows the percentages of dominant trajectories of all vertices. We observe that this ratio is below 0.2 for most vertices, especially when the vertex is traversed by a relatively large number of trajectories (e.g., greater than 10,000). For TPMFP queries over Year Dataset, the above results demonstrate that CFMI can reduce the number of random disk accesses by a factor of 5 compared with FMI.

6.3.3 Query Performance of TPMFP

The response time of an TPMFP query consists of two parts, namely the time of constructing the footmark graph and the time of searching the MFP in the footmark graph.

To evaluate the time of footmark graph construction, we compare three algorithms including Algorithm 2, Algorithm 3 and an algorithm that performs full scan on all trajectories. Moreover, we consider three memory modes. The *Tiny-Dataset mode* loads all trajectories and indexes into memory to avoid any disk access. The *Small-Dataset mode* loads all trajectories and part of the indexes including all dominant trajectory tables (CFMI only) and all non-leaf B^+-tree nodes into memory. The *Big-Dataset mode* differs from the Small-Dataset mode in that it does not load trajectories into memory. In this experiment, we fix the destination and use different time periods to vary the number of trajectories involved. The performance of footmark graph construction on Month Dataset is shown in Figure 13. We can see that the algorithm using CFMI outperforms the other two in all cases. For both FMI and CFMI, the footmark construction time is increasing linearly with the number of trajectories.

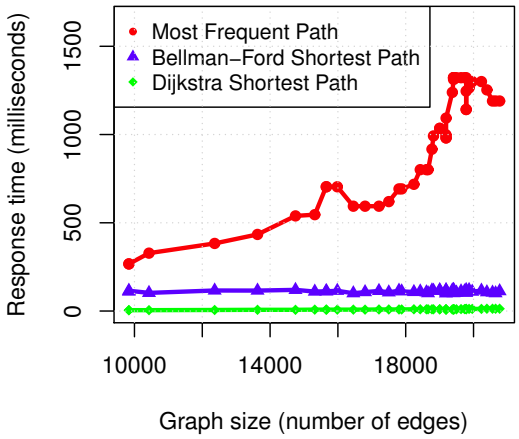

Figure 12: Performance of searching MFP on a footmark graph

The footmark construction time using CFMI on Year Dataset is depicted in Figure 11. The destination is set to the busiest road intersection, i.e., the vertex with the greatest number of trajectories passed through. Therefore, the result can reflect the worst cases among all possible queries. We can see that our algorithm takes less than 40 seconds to construct the largest footmark graph, which is fairly efficient for a dataset containing over 11.5 million trajectories.

Once the footmark graph is created, the MFP searching algorithm will be executed in memory. The performance of Algorithm 4 is only affected by the size of the graph, which is depicted in Figure 12. The result shows that searching MFP is slower than searching the shortest path. The reason is that the computation complexity of updating vertex status in the MFP algorithm is $O(\alpha)$, which is higher than that in the other two algorithms ($O(1)$). However, for big datasets, the performance of MFP searching algorithm is not critical as the execution time of the whole TPMFP query is dominated by the footmark construction.

6.3.4 TPMFP vs. Time Period-Based MPR

Since the original MPR algorithm does not deal with user-specified time periods, it performs a lot of time-consuming pre-computations and saves the results for future MPR queries. When dealing with dynamic time periods, these pre-computations must be performed in an online manner, which leads to extremely slow response time. For example, we conduct a rough comparison using Month Dataset with T set to the whole month. The response time of 'time period-based MPR' is around 200 seconds, while the TPMFP algorithm takes less than 1 second.

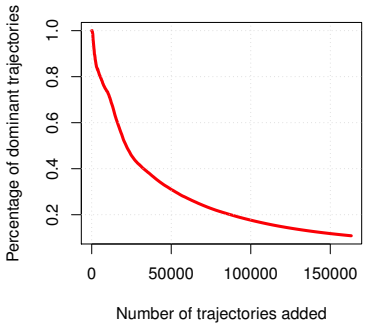

Figure 9: The decreasing trend of percentages of dominant trajectories

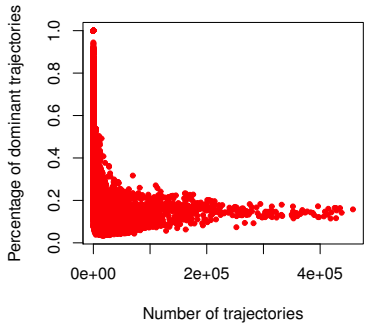

Figure 10: Percentages of dominant trajectories of all vertices

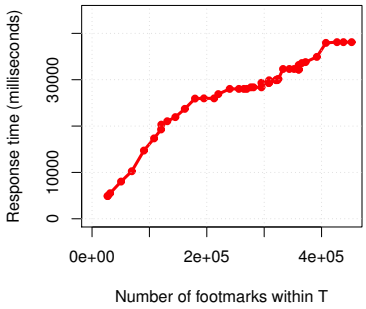

Figure 11: Footmark graph construction time using CFMI (Year Dataset)

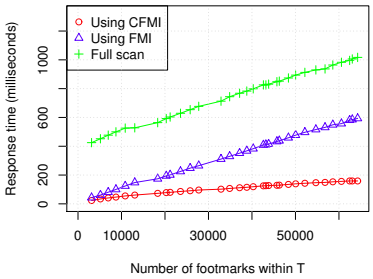

(a) Tiny-Dataset Mode

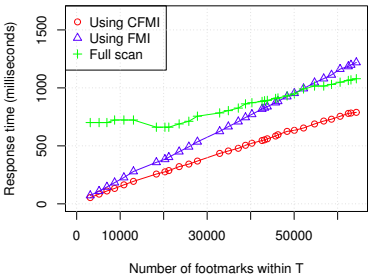

(b) Small-Dataset Mode

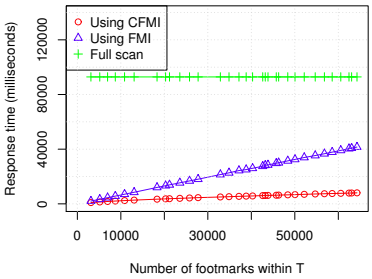

(c) Big-Dataset Mode

Figure 13: Footmark graph construction time using different approaches (Month Dataset)

7. RELATED WORK

Finding the most desirable path has received tremendous research interests for decades. The most popular topic in this area is shortest path finding [6, 1, 22], which has been extensively studied for over fifty years. If the weight on each edge represents travel time, shortest path finding becomes fastest path finding. Time-dependent shortest path problem [7, 13, 21] regards the travel time of an edge as a single-valued function on time of day. To improve routing services, new approaches [11, 29, 30] for fastest path finding are proposed aiming at using user-generated GPS trajectories to estimate the distribution of travel time on a given road network. Unlike shortest/fastest path finding, our work studies the desirability of a path from a different perspective, i.e., how frequently the path has been taken during a certain time period.

Popular route searching [3, 27] is the most closely related work to the TPMFP problem. Zaiben et al [3] are the first to study the common routing preferences of the past travelers. Utilizing historical trajectory datasets, it proposes a novel popularity function for path desirability evaluation. However, this method tends to favor the paths with fewer vertices. Moreover, the most popular route (MPR) may contain least frequent edges. The work in [27] aims at finding top-k popular routes from uncertain trajectories. Assuming that there is no map at hand, they focus on deriving routes from uncertain trajectory data. They calculate the popularity of each edge by simply counting the number of trajectories traversed it, without considering whether they have passed through the specified destination. It is therefore not suitable for the application scenarios of the TPMFP problem. Note that both of these works only consider the fixed time range, while the TPMFP problem can be carried out in arbitrary time periods specified by the users.

Hot route and trajectory pattern detection also try to reflect the common routing behaviors of the past travelers. Informally, a hot route is a path with heavy traffic. Various trajectory clustering approaches [16, 15, 9, 14] can be utilized to discover hot routes. In [24], an online algorithm is developed to detect the hot motion paths that have been frequently traversed by the past travelers. Similar to hot routes, trajectory patterns represent the frequent travel behaviors in terms of both time and locations. Typical approaches for trajectory pattern mining include T-pattern mining [10], periodic pattern mining [19], interesting locations and travel sequences mining [33], etc. Unlike the problem of TPMFP, these approaches find the desired hot routes/trajectory patterns in a global manner and no specific source and destination are considered. They are therefore not suitable for finding the MFP from a specified location to another.

Another relevant problem to our work is the management of trajectory data. So far, a number of data access methods, which are variants of R-tree [12], have been proposed for moving object trajectories. Typical examples include 3D R-trees [26], MR-trees [28], HR-trees [20], MV3R-trees [25], TB-trees [23], SETI [2], TrajStore [4], FNR-trees [8] and MON-trees [5]. In particular, FNR-trees and MON-trees are designed for indexing trajectories that have already been matched to a road network. However, these structures are not suitable for efficient footmark retrieving due to two reasons. First, the query of footmarks is much more complex than the ones (e.g., window/range queries and timestamp/interval queries) that these structures are primarily designed for. Second, they become inefficient when the results are very large. In our work, we proposed special techniques (e.g., CFMI) to calculate most of the results instead of fetching them all from disk.

8. CONCLUSION

In this paper, we study the problem of TPMFP, i.e, finding the time period-based most frequent path. We propose a novel definition of TPMFP which satisfies three key properties, namely suffix-optimal, length-insensitive and bottleneck-free. This is a new query and the definition of TPMFP well reflects the people's common sense notion. Moreover, we devise a two-step framework to efficiently perform TPMFP queries on very large trajectory datasets. The first step is to construct a footmark graph which can be used to calculate the frequencies of the candidate paths. To this end, we propose two novel indexing schemes to reduce the number of random disk accesses. The second step is to search the most frequent path in the footmark graph and an efficient algorithm is proposed. In addition, we conduct extensive experiments using a real big trajectory dataset containing 11.5 million trajectories. The results demonstrate the effectiveness and the efficiency of our index schemes and algorithms.

Acknowledgement

This research was supported in part by Hong Kong, Macao and Taiwan Science & Technology Cooperation Program of China under Grant 2012DFH10010, Science and Technology Planning Project of Guangzhou China under Grant 2012Y2-00030, Huawei Corp. Contract YBCB2009041-27, Huawei Corp. Contract HWLB06-15C03212/13PN, Hong Kong RGC GRF Project No.611411, National Grand Fundamental Research 973 Program of China under Grant 2012-CB316200, HP IRP Project, and Microsoft Research Asia Grant.

9. REFERENCES

[1] R. Bellman. On a routing problem. *Quarterly of Applied Mathematics*, 16:87–90, 1958.

[2] V. P. Chakka, A. Everspaugh, and J. M. Patel. Indexing large trajectory data sets with seti. In *CIDR*, 2003.

[3] Z. Chen, H. T. Shen, and X. Zhou. Discovering popular routes from trajectories. In *ICDE*, pages 900–911, 2011.

[4] P. Cudré-Mauroux, E. Wu, and S. Madden. Trajstore: An adaptive storage system for very large trajectory data sets. In *ICDE*, pages 109–120, 2010.

[5] V. T. De Almeida and R. H. Güting. Indexing the trajectories of moving objects in networks*. *Geoinformatica*, 9(1):33–60, 2005.

[6] E. W. Dijkstra. A note on two problems in connexion with graphs. *Numerische mathematik*, 1(1):269–271, 1959.

[7] B. Ding, J. X. Yu, and L. Qin. Finding time-dependent shortest paths over large graphs. In *EDBT*, pages 205–216, 2008.

[8] E. Frentzos. Indexing objects moving on fixed networks. In *SSTD*, pages 289–305, 2003.

[9] S. Gaffney and P. Smyth. Trajectory clustering with mixtures of regression models. In *SIGKDD*, pages 63–72, 1999.

[10] F. Giannotti, M. Nanni, F. Pinelli, and D. Pedreschi. Trajectory pattern mining. In *SIGKDD*, pages 330–339, 2007.

[11] H. Gonzalez, J. Han, X. Li, M. Myslinska, and J. P. Sondag. Adaptive fastest path computation on a road network: a traffic mining approach. In *VLDB*, pages 794–805, 2007.

[12] A. Guttman. R-trees: a dynamic index structure for spatial searching. In *SIGMOD*, pages 47–57, 1984.

[13] E. Kanoulas, Y. Du, T. Xia, and D. Zhang. Finding fastest paths on a road network with speed patterns. In *ICDE*, pages 10–, 2006.

[14] J.-G. Lee, J. Han, X. Li, and H. Gonzalez. Traclass: trajectory classification using hierarchical region-based and trajectory-based clustering. *PVLDB*, 1(1):1081–1094, 2008.

[15] J.-G. Lee, J. Han, and K.-Y. Whang. Trajectory clustering: a partition-and-group framework. In *SIGMOD*, pages 593–604, 2007.

[16] X. Li, J. Han, J.-G. Lee, and H. Gonzalez. Traffic density-based discovery of hot routes in road networks. In *SSTD*, pages 441–459, 2007.

[17] Z. Li, B. Ding, J. Han, and R. Kays. Swarm: mining relaxed temporal moving object clusters. *Proc. VLDB Endow.*, 3(1-2):723–734, 2010.

[18] Y. Lou, C. Zhang, Y. Zheng, X. Xie, W. Wang, and Y. Huang. Map-matching for low-sampling-rate gps trajectories. In *ACM SIGSPATIAL GIS*, pages 352–361, 2009.

[19] N. Mamoulis, H. Cao, G. Kollios, M. Hadjieleftheriou, Y. Tao, and D. W. Cheung. Mining, indexing, and querying historical spatiotemporal data. In *SIGKDD*, pages 236–245, 2004.

[20] M. A. Nascimento and J. R. O. Silva. Towards historical r-trees. In *SAC*, pages 235–240, 1998.

[21] A. Orda and R. Rom. Shortest-path and minimum-delay algorithms in networks with time-dependent edge-length. *J. ACM*, 37(3):607–625, 1990.

[22] S. Pallottino and M. G. Scutella. Shortest path algorithms in transportation models: classical and innovative aspects. *Equilibrium and advanced transportation modelling*, 245:281, 1998.

[23] D. Pfoser, C. S. Jensen, and Y. Theodoridis. Novel approaches in query processing for moving object trajectories. In *VLDB*, pages 395–406, 2000.

[24] D. Sacharidis, K. Patroumpas, M. Terrovitis, V. Kantere, M. Potamias, K. Mouratidis, and T. Sellis. On-line discovery of hot motion paths. In *EDBT*, pages 392–403, 2008.

[25] Y. Tao and D. Papadias. Mv3r-tree: A spatio-temporal access method for timestamp and interval queries. In *VLDB*, pages 431–440, 2001.

[26] Y. Theodoridis, M. Vazirgiannis, and T. Sellis. Spatio-temporal indexing for large multimedia applications. In *ICMCS*, pages 441–448, 1996.

[27] L.-Y. Wei, Y. Zheng, and W.-C. Peng. Constructing popular routes from uncertain trajectories. In *ACM SIGKDD*, pages 195–203, 2012.

[28] X. Xu, J. Han, and W. Lu. Rt-tree: An improved r-tree index structure for spatiotemporal. *SDH*, pages 1040–1049, 1990.

[29] J. Yuan, Y. Zheng, X. Xie, and G. Sun. Driving with knowledge from the physical world. In *SIGKDD*, pages 316–324, 2011.

[30] J. Yuan, Y. Zheng, C. Zhang, W. Xie, X. Xie, G. Sun, and Y. Huang. T-drive: driving directions based on taxi trajectories. In *SIGSPATIAL GIS*, pages 99–108, 2010.

[31] J. Yuan, Y. Zheng, L. Zhang, X. Xie, and G. Sun. Where to find my next passenger. In *UbiComp*, pages 109–118, 2011.

[32] Y. Zheng, Y. Liu, J. Yuan, and X. Xie. Urban computing with taxicabs. In *UbiComp*, pages 89–98, 2011.

[33] Y. Zheng, L. Zhang, X. Xie, and W.-Y. Ma. Mining interesting locations and travel sequences from gps trajectories. In *WWW*, pages 791–800, 2009.